Zinc Phthalocyanine Thin Film-Based Optical Waveguide H$_2$S Gas Sensor

Kediliya WUMAIER[1], Gulgina MAMTMIN[2], Qingrong MA[1],
Asiya MAIMAITI[1], Patima NIZAMIDIN[1], and Abliz YIMIT[1*]

[1]*College of Chemical Engineering, Xinjiang University, Urumqi 830046, China*

[2]*College of Chemistry and Environmental Science, Kashgar University, Kashgar 844006, China*

*Corresponding author: Abliz YIMIT   E-mail: ablizy@sina.com

Abstract: The detection of hydrogen sulfide (H$_2$S) is essential because of its toxicity and abundance in the environment. Hence, there is an urgent requisite to develop a highly sensitive and economical H$_2$S detection system. Herein, a zinc phthalocyanine (ZnPc) thin film-based K$^+$-exchanged optical waveguide (OWG) gas sensor was developed for H$_2$S detection by using spin coating. The sensor showed excellent H$_2$S sensing performance at room temperature with a wide linear range (0.1 ppm $-$ 500 ppm), reproducibility, stability, and a low detection limit of 0.1 ppm. The developed sensor showed a significant prospect in the development of cost-effective and highly sensitive H$_2$S gas sensors.

Keywords: Zinc phthalocyanine thin film; optical waveguide; H$_2$S detection; protonation

1. Introduction

Hydrogen sulfide (H$_2$S) is a colorless gas with pungent odor and is usually produced during the decomposition of organic matter, smelting, waste-water treatment, and landfill designing. As an air pollutant, H$_2$S seriously affects human health and has been classified as a toxic and dangerous chemical by occupational safety and health standards. Low concentrations of H$_2$S gas can damage the human respiratory and nervous systems, while long-term or high-level exposure can cause dizziness, vomiting, and even death [1]. Therefore, the detection of H$_2$S gas has gained immense scientific attention and it is imperative to develop a H$_2$S gas sensor with high-efficiency, low detection limit, and quick response.

A variety of gas sensors such as electrochemical [2, 3], piezoelectric [4], metal oxide semiconductor-based [5–7], micro-electro-mechanical based system [8], and optical waveguide (OWG) sensors [9, 10] have been developed to detect H$_2$S gas.

The waveguide (WG) technology is well developed and can be utilized in gas sensors. Huang *et al.* [11] proposed an evanescent field-absorption gas sensor based on the silicon-on-sapphire WG in the mid-IR (infrared) wavelength region to detect fluctuations in CO$_2$ concentration at the atmospheric base level.

Kazanskiy *et al.* [12] proposed a novel polarization-insensitive hybrid plasmonic WG design, which corresponded to the absorption line of the deadly methane gas. Khonina *et al.* [13] presented a more sensitive dual hybrid plasmonic WG structure for the detection of methane gas. Ranacher *et al.* [14] presented a photonic gas sensor concept based on a silicon WG by using infrared evanescent field absorption, and quantitative measurements of CO$_2$ were conducted for concentrations as low as 500 ppm CO$_2$.

WG sensors have numerous attractive features, such as high sensitivity, fast response, and room temperature operation, as listed in Table 1. The OWG sensor is based on the principle of evanescent waves. An optical waveguide is generally composed of a cladding layer (refractive index, n_c), a waveguide layer (n_f), and a substrate (n_s). In the waveguide structure, when $n_f > n_s > n_c$, the light undergoes total internal reflection during propagation in the wave guide layer. The light wave penetrates into a very thin layer of the second medium and undergoes a Goos-Hänchen shift before returning to the first medium layer. The light wave that penetrates the second medium is called an evanescent wave.

Table 1 Different OWGs used for H$_2$S sensing.

Sensing material	Low detection limit (ppm)	Response time	Operation temperature	Ref.
Chitosan/Au and chitosan/Ag nanocomposites	0.1	Within a few minutes	Room temperature	[15]
Au-doped ZnFe$_2$O$_4$ yolk shell microspheres film	200	46 s	Room temperature	[16]
Ahionine dye–polyvinyl alcohol film	0.1	<2 s	Room temperature	[17]
Tetracarboxyl-phenyl porphyrin hybridized graphitic carbon nitride film	1	6 s	Room temperature	[18]
ZnPc film	0.1	3 s	Room temperature	This work

Phthalocyanines (Pcs), especially metal Pcs show high photo- and thermal stability due to their 18-π conjugated electron system composed of carbon-nitrogen conjugated double bonds. As a class of macrocyclic planar aromatic compounds, MPcs are promising organic compounds with a huge potential for the application in electro-optical devices [19], photodynamic therapy [20, 21], catalysts [22], nonlinear optics [23], and gas sensors [24–26].

Zinc phthalocyanine (ZnPc) has received significant attention in the optical field due to its excellent nonlinear optical properties, such as high light absorption coefficient in the visible region, high triplet quantum yield, and high lifetime [27, 28]. Gas sensors based on ZnPc organic semiconductors have recently become noticeable because of their inherent advantages [29, 30]. Yet, studies on ZnPc-based materials such as OWG sensors remain limited. In this work, we reported that a highly sensitive and cost-effective ZnPc thin film-based K+-exchanged OWG gas sensor was developed for H$_2$S detection. In this study, we fabricated ZnPc thin films by using spin coating with different rotation speeds and different mass fractions of ZnPc. The influence of coating conditions on the gas sensing properties of the films were examined. The principles of the sensing and stability of the film-based sensors were discussed.

2. Experiment

2.1 Reagents and instrumentation

ZnPc was purchased from Shanghai Bailingwei Chemical Technology Co., Ltd. Polyvinyl pyrrolidone (PVP) was purchased from Tianjin Bodi Chemical Technology Co., Ltd. A DHG-9023A vacuum drying chamber (Shanghai-Hengke), along with a KW-4A spin coater (Shanghai Kaimeite Artificial China Technology), was used for film coating. A gas detection tube was also employed (working range: 2 ppm to 200 ppm, Gastec, Beijing

Municipal Institute, Beijing, China), together with a homemade OWG testing system.

2.2 Preparation of volatile organic compounds and H_2S

Volatile organic compounds (VOCs) were obtained by using a natural volatilization method. A specific amount of organic solvent was added to a 600 mL container with a micro syringe and left to volatilize naturally for 3 h after sealing.

H_2S was obtained by the reaction of ferrous sulfide (FeS) and concentrated hydrochloric acid (HCl). A specific amount of FeS was weighted into a 600 mL container, followed by the addition of a controlled volume of HCl.

The different concentrations of gases were obtained by using the dilution method. The concentrations of the prepared gases were determined by using a gas detection tube, and the results were consistent with the calculated values.

2.3 Preparation of the K^+-exchanged OWG component

The K^+ ion exchanged OWGs were prepared by using a thermo-ionic diffusion method. Firstly, potassium nitrate (KNO_3) powder was fused in a muffle furnace at 400 ℃. A clean glass slide was then immersed in the molten KNO_3 to induce ion exchange. After 40 min, the Na^+ ions on the glass surface were exchanged with the K^+ ions and cooled to room temperature. The cooled glass slide was then washed several times with distilled water and absolute ethanol, and reserved for later use.

2.4 Fabrication of ZnPc thin film-based OWG sensitive element

ZnPc (sensitive material) and PVP (film former) were dissolved (in the desired amounts) in 10 mL N,N-dimethylformamide (DMF) to obtain a ZnPc solution. This solution was coated on the surface of a K^+-exchanged glass slide by spin coating. The as-fabricated sensor was dried under vacuum for 24 h at room temperature. The fabricated film was

characterized by using ultraviolet spectrophotometry (UV-1780 ultraviolet spectrophotometer, SHIMADZU, Japan), field emission scanning electron microscopy (FE-SEM, SU-8019, Japan Hitachi), and Fourier-transform infrared spectrometry (FT-IR, Bruker Co., Germany).

2.5 OWG testing system

The homemade OWG gas detection system used in this study consisted of a laser, a reflector, chamber (2 cm × 1 cm × 1 cm), a ZnPc thin film-based OWG gas-sensing element, a prism, photomultiplier, a personal computer, and a carrier (air) (Fig. 1).
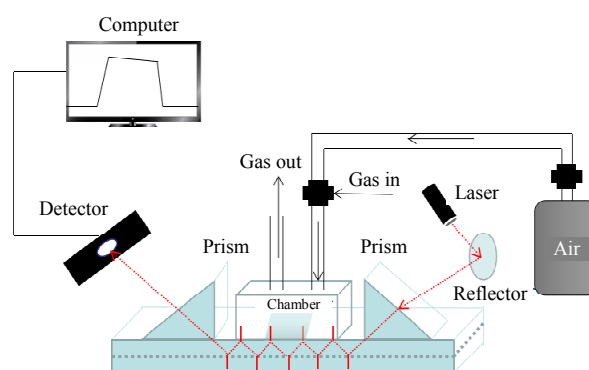

Fig. 1 OWG testing system.

In general, the ZnPc thin film-based sensitive element was fixed in the OWG detection system (Fig. 1) and a prism coupling method was used to excite guided light. In the gas detection process, dry air with a flow rate of 30 cm^3/min was used as a carrier gas which was injected into the flow cell before the target gas to ensure the complete contact of the sensitive film with the target gas. A few drops of diiodomethane [CH_2I_2, (refractive index) $n = 1.74$] were added to adhere the prism to the surface of the glass optical waveguide element. When a semiconductor laser beam with a wavelength of 670 nm entered the surface of the OWG sensitive element through the first prism, the light entered the sensitive layer in the form of evanescent wave [31]. When the sensitive element interacted with the measured gas, it caused a change in the optical

performance of the sensitive element and the form of propagation of the evanescent wave, thereby causing a change in the output light intensity. The light output by the second prism was transmitted to the photomultiplier tube and converted into an electrical signal. The changes in the output light intensity with time were recorded by the computer.

3. Results and discussion

3.1 Characterization

3.1.1 UV-vis measurements

In general, Pcs have two main characteristic peaks in the ultraviolet-visible (UV-vis) spectrum, which are the B band of 300 nm – 400 nm and the Q band of 600 nm – 700 nm [32]. These two absorption peaks are caused by the transition of π electrons on the phthalocyanine ring, and the Q band is the main concern in practical applications [33].

Figure 2 shows the UV-vis spectra of the ZnPc solution in DMF and the ZnPc thin film. The Q-bands of the ZnPc solution and ZnPc thin film were observed at 668 nm and 678 nm, respectively. Compared with the ZnPc solution, the ZnPc thin film Q-band showed a red-shift for approximately 10 nm. This phenomenon could be attributed to the formation of J-aggregates in the thin film [34]. Pc molecules formed two types of aggregates, H- and J-aggregates. J-aggregates exhibited better photoelectric properties than H-aggregates because of their higher dipole moment [35].

3.1.2 SEM measurements

Generally, the gas sensitivity of the film is closely related to its surface morphology. Thus, the surface morphology of the ZnPc thin film was examined at different magnifications by field emission scanning electron microscopy (FE-SEM). It is evident from Fig. 3(a) that ZnPc molecules existed as small particles and the average particle

size of the particles was 10 nm. Moreover, from Fig. 3(b), it could be seen that the ZnPc thin film had a smooth and dense structure.
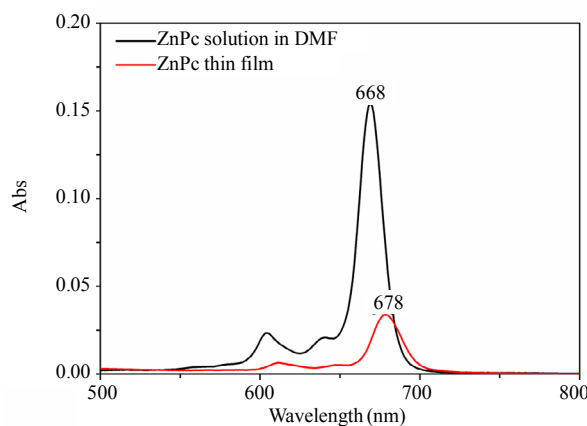

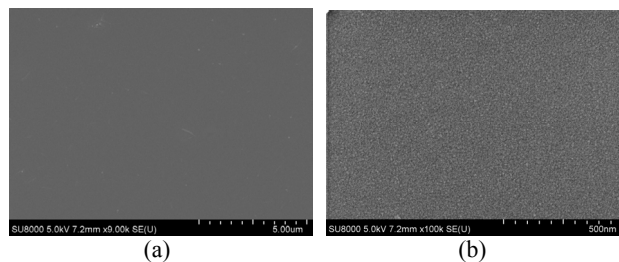Fig. 2 UV-vis absorption spectra of the ZnPc solution and ZnPc thin film.

Fig. 3 FE-SEM images of the ZnPc thin film at low (a) and high (b) magnifications.

3.1.3 FT-IR spectroscopy

The FT-IR spectra of ZnPc before and after contacting with H$_2$S were measured. The results are shown in Fig. 4. It is evident from the figure that after contacting with H$_2$S, the characteristic absorption peaks of ZnPc had a tendency to move to high wave numbers. This phenomenon could be attributed to the higher symmetry of ZnPC after contacting with H$_2$S.

3.2 Gas sensing performance

To choose a suitable light source for the OWG testing system, the ZnPc thin film was exposed to 1 000 ppm of measured gases and the changes in absorbance were monitored. The maximum changes in absorbance were caused by H$_2$S (Fig. 5). Figure 5 shows that after contacting with H$_2$S gas, the absorbance of the film was greatly reduced and the

Q band had a significant split and a red shift. This trend was most significant in the range of 600 nm – 800 nm, therefore a 670 nm semiconductor laser was used as the light source.
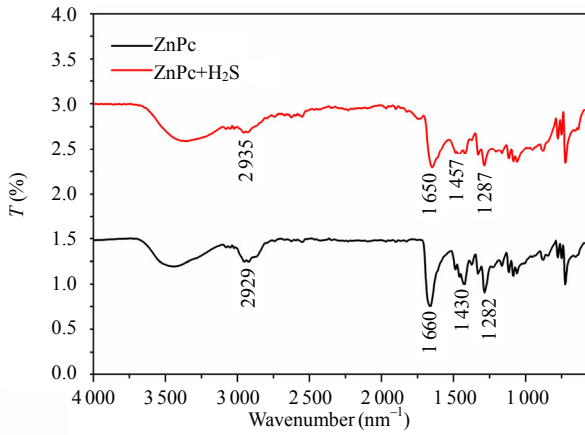

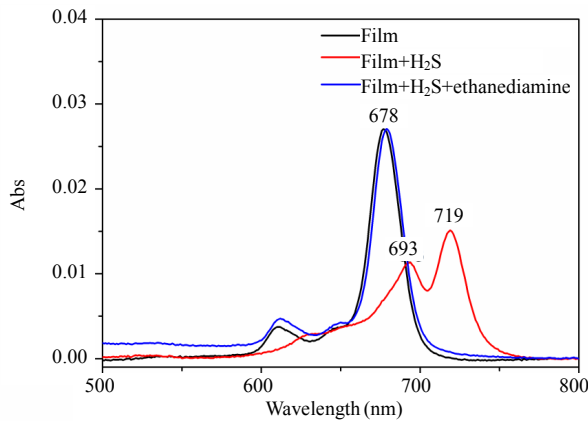Fig. 4 FT-IR spectroscopy of the ZnPc before and after contacting with H_2S.

Fig. 5 Changes in absorbance of the ZnPc thin film before and after contacting with H_2S gas.

Figure 6 shows results for the optimization of the fabrication conditions. The screening results for the rotation speed, ZnPc mass fraction, and PVP content are listed in Table 2.

In Fig. 6, ΔI denotes the change in the output light intensity and is calculated using the following formula [36]:

$$\Delta I \text{(signal intensity change)} = I_{gas} - I_{air}$$

where I_{gas} is the output light intensity of the gas and I_{air} is the output light intensity of the surrounding air.

From Fig. 6, it can be seen that the ZnPc thin film OWG prepared with a 1 600 rpm of rotating

speed (Table 3), 0.07% ZnPc mass fraction (Table 4), and 1.0% PVP content (Table 5) exhibited the greatest sensing response to H_2S. Therefore, it was confirmed to be the optimum condition for the fabrication of the ZnPc thin film. Moreover, it is
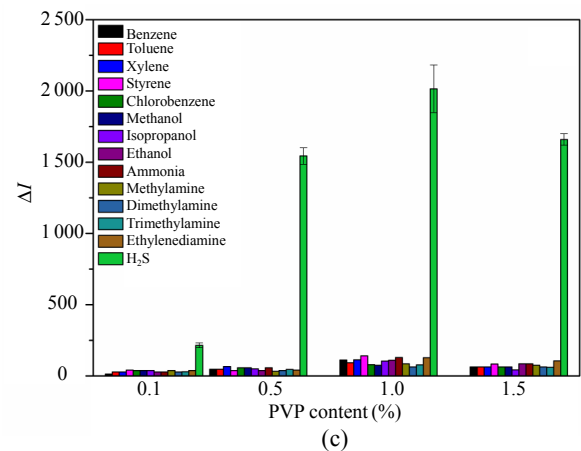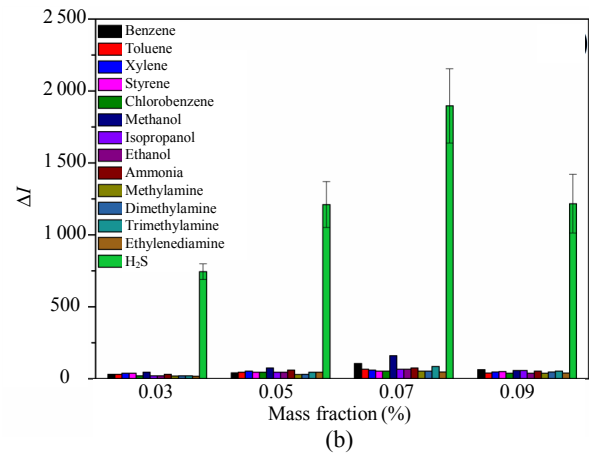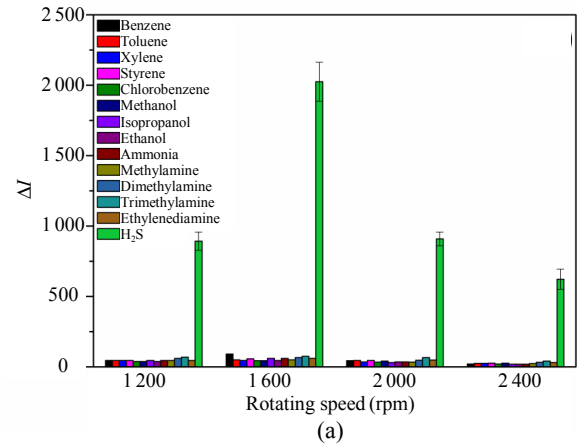

Fig. 6 Optimization of the fabrication conditions: (a) rotating speed, (b) mass fraction of ZnPc, and (c) PVP content.

Table 2 Fabrication conditions of the sensitive element.

Rotating speed (rpm)	1 200	1 600	2 000	2 400
Mass fraction of the ZnPc solution (%)	0.03	0.05	0.07	0.09
PVP content (%)	0.1	0.5	1.0	1.5

clear that the response of the sensor to H₂S was higher than that of other gases, which was consistent with the results of UV-vis spectroscopy. This indicated an appreciable selectivity for H₂S. In each table, Numbers 1 – 13 represent benzene, toluene, xylene, styrene, chlorobenzene, methanol, isopropanol, ethanol, ammonia, methylamine, dimethylamine, trimethylamine, and ethylenediamine, and Number 14a represents the mean value of H₂S and Number 14b represents the standard deviation. Gas concentrations for all VOCs (Numbers 1 – 13) were 1 000 ppm, and the gas concenreation of H₂S is 100 ppm.

Table 3 Measured values of H₂S and other VOCs under different rotating speeds.

	1	2	3	4	5	6	7	8	9	10	11	12	13	14a	14b
1 200 rpm	46	46	46	46	38	38	46	38	46	46	61	69	46	892.00	64.58
1 600 rpm	92	51	46	58	45	45	61	46	61	50	66	75	61	2024.33	138.96
2 000 rpm	45	46	36	46	34	42	31	35	35	34	48	66	49	908.67	48.01
2 400 rpm	21	25	25	27	21	27	19	20	20	24	32	42	31	622.33	71.22

Table 4 Measured values of H₂S and other VOCs under different mass fractions.

	1	2	3	4	5	6	7	8	9	10	11	12	13	14a	14b
0.03%	31	31	39	39	21	46	21	21	31	19	21	21	18	743.67	54.20
0.05%	41	46	53	46	46	76	46	46	61	30	31	46	46	1211.00	159.32
0.07%	106	67	61	54	53	161	67	67	76	53	54	86	48	1896.67	258.00
0.09%	64	40	48	50	38	58	57	39	53	38	48	53	40	1217.00	204.50

Table 5 Measured values of H₂S and other VOCs under different PVP contents.

	1	2	3	4	5	6	7	8	11	10	11	12	13	14a	14b
0.1%	14	28	29	42	38	38	38	29	28	38	28	30	39	215.67	17.56
0.5%	48	47	67	38	57	57	51	39	38	33	38	46	42	1543.67	57.50
1.0%	112	93	114	141	79	76	105	110	64	85	64	78	128	2015.33	166.13
1.5%	63	63	63	84	63	63	43	85	63	76	63	60	106	1659.33	40.55

Figure 7 shows the selective response of the sensor prepared under optimal conditions to 1 000 ppm of VOCs (a) and 100 ppm of H₂S (b). The response of the sensor to VOCs was very small [Fig. 7(a)], and the sensor exhibited the largest response to H₂S because of the protonation interactions [Fig. 7(b)]. The protonation process could be used to explain the absorption change (Fig. 8).
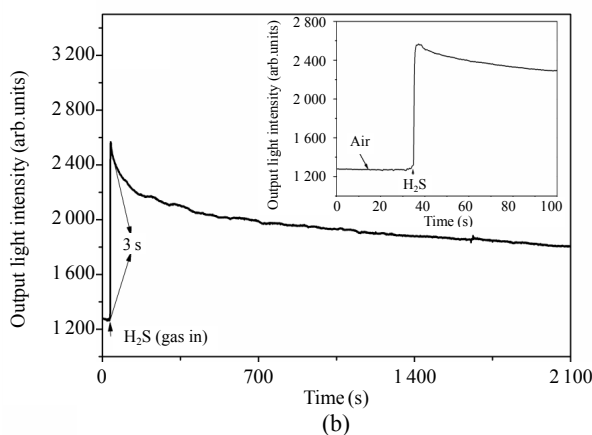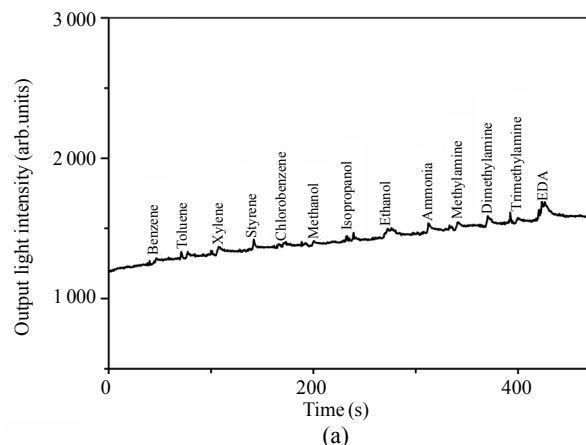

Fig. 7 Dynamic response curve of the ZnPc thin film-based sensor to (a) 1 000 ppm VOCs and (b) 100 ppm H₂S.
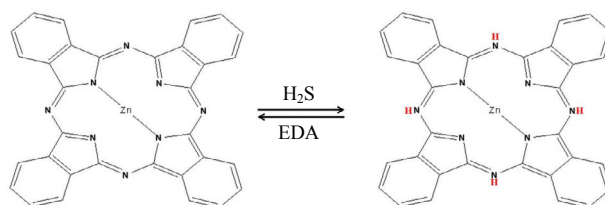

Fig. 8 Sensing mechanism of the ZnPc.

As the pyrrolic and azomethine (meso) nitrogen atoms in Pc exhibited acidic and basic characteristics, respectively, it was an amphoteric molecule. Unprotonated MPcs exhibited D₄ₕ

symmetry. However, the symmetry decreases after protonation, causing the splitting and red-shifting of the Q band [37]. In addition, upon exposure to ethylenediamine (EDA)-saturated vapor, the absorption spectrum of the film returned to its initial unprotonated state. These results indicated that the ZnPc thin film could be protonated by H_2S (acidic substance) and deprotonated by EDA (basic substance). From Fig. 7(b), it is evident that after contacting with H_2S, the response time was 3 s, but the response value did not recover automatically to the baseline because of the irreversible protonation process.

According to Fig. 9, when the sensor is in contacting with H_2S, the response value increased rapidly. After the response value attained the maximum value, it began to recover. However, owing to irreversible protonation, the response value could not return to the baseline in a short time. However, the response value could be returned to the baseline by contacting with saturated EDA. By using this technique, every H_2S response-recovery process is repeatable. The relative standard deviation (RSD) value was 2.6%.
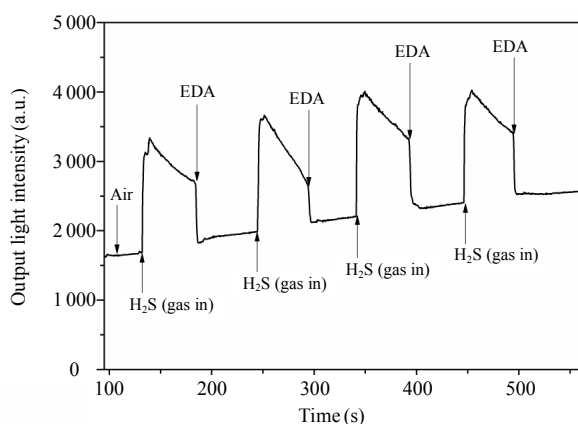

Fig. 9 Dynamic response curve of repeatable protonation-deprotonation process of the ZnPc thin-film based sensor to 100 ppm of H_2S.

Figure 10 shows a low concentration of H_2S detection by using the ZnPc thin film-based sensor. As observed from Fig. 10, the output light intensity increased with an increase in the H_2S concentration. The sensor could detect as low as 0.1 ppm of H_2S

($S/N = 3.6$).

Figure 11 shows a scatter plot for different H_2S concentrations and the corresponding ΔI values. The linear relationship was $y = 532x + 4424$, $R^2 = 0.9823$.

The long-term stability of the ZnPc thin film-based sensor was studied by exposure to 100 ppm of H_2S after 1 day, 7 days, 14 days, 21 days, and 28 days of its fabrication. The results are shown in Fig. 12. A small change was observed in the gas sensing performance of the sensor during this period. The RSD value of the sensor was 2.6%. These results demonstrated the long-term stability and reproducibility of the sensor.
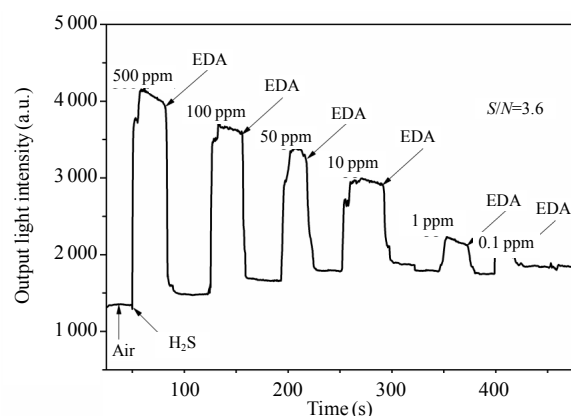

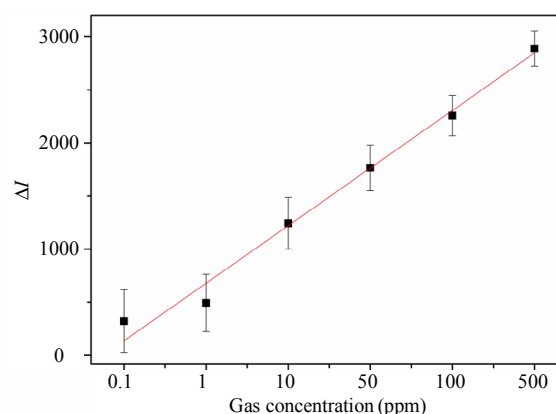Fig. 10 Typical response of the ZnPc thin film-based sensor when exposed to different concentrations of H_2S.

Fig. 11 Scatter plot for different H_2S concentrations and corresponding ΔI values.

The stability against humidity variation was also studied. Different saturated salt solutions were

prepared to obtain different humidities (Table 6). The results are shown in Fig. 13. From the effect of different humidities on the sensor, it could be considered that the change in humidity had little effect on the sensor.
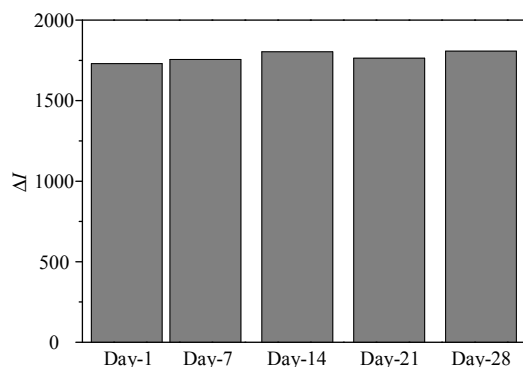

Fig. 12 Histogram of H$_2$S gas (100 ppm) sensing performance of the sensor after 1 day, 7 days, 14 days, 21 days, and 28 days of its fabrication.

Table 6 Relative humidity of saturated salt solutions.

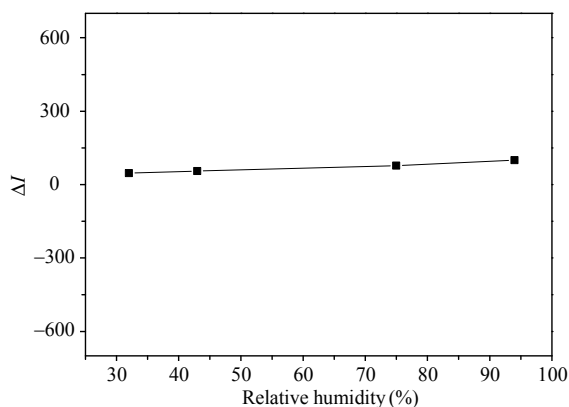| Saturated salt solution (25℃)	Humidity (%)
MgCl$_2$	32
K$_2$CO$_3$	43
NaCl	75
KNO$_3$	94

Fig. 13 Effect of the relative humidity on sensor.

4. Conclusions

In this study, a novel ZnPc thin film-based OWG gas sensor was fabricated and its gas sensing performance was studied. The fabricated OWG sensor showed a high selectivity to H$_2$S due to protonation. The ZnPc thin film-based OWG sensor was able to detect H$_2$S at a level of 100 ppb. The sensor also showed the good reproducibility, stability, and fast response. The low cost, easy implementation, and high sensitivity of this sensor make it suitable for many environmental and chemical applications.

Acknowledgment

References

[1] F. I. M. Ali, F. Awwad, Y. E. Greish, and S. T. Mahnoud, "Hydrogen sulfide (H$_2$S) gas sensor: a review," *IEEE Sensors Journal*, 2018, 19(7): 2394–2407.

[2] X. D. Hao, C. Ma, X. Yang, T. Liu, B. Wang, F. M. Liu, *et al.*, "YSZ-based mixed potential H$_2$S sensor using La$_2$NiO$_4$ sensing electrode," *Sensors and Actuators B: Chemical*, 2018, 255: 3033–3039.

[3] V. Balasubramani, S. Sureshkumar, T. Rao, and T. M. Sridhar, "Impedance spectroscopy-based reduced graphene oxide-incorporated ZnO composite sensor for H$_2$S investigations," *ACS Omega*, 2019, 4(6): 9976–9982.

[4] R. Kitture, D. Pawar, C. N. Rao, R. K. Choubey, and S. N. Kale, "Nanocomposite modified optical fiber: a room temperature, selective H$_2$S gas sensor: studies using ZnO-PMMA," *Journal of Alloys and Compounds*, 2017, 695: 2091–2096.

[5] J. Sarfraz, P. Ihalainen, A. Maattanen, T. Gulin, J. Koskela, C. E. Wilen, *et al.*, "A printed H$_2$S sensor with electro-optical response," *Sensors and Actuators B: Chemical*, 2014, 191: 821–827.

[6] Y. X. Nie, P. Deng, Y. Y. Zhao, P. L. Wang, L. L. Xing, Y. Zhang, *et al.*, "The conversion of PN-junction influencing the piezoelectric output of a CuO/ZnO nanoarray nanogenerator and its application as a room-temperature self-powered active H$_2$S sensor," *Nanotechnology*, 2014, 25(26): 265501.

[7] J. T. Zhang, Z. J. Zhu, C. M. Chen, Z. Chen, M. Q.

Cai, B. H. Qu, *et al.*, "ZnO-carbon nanofibers for stable, high response, and selective H₂S sensors," *Nanotechnology*, 2018, 29(27): 275501.

[8] M. He, L. L. Xie, X. L. Zhao, X. B. Hu, S. H. Li, and A. G. Zhu, "Highly sensitive and selective H₂S gas sensors based on flower-like WO₃/CuO composites operating at low/room temperature," *Journal of Alloys and Compounds*, 2019, 788: 36–43.

[9] A. Maimaiti, R. Abdurahman, N. Kari, Q. R. Ma, K. Wumaier, P. Nizamidin, *et al.*, "Highly sensitive optical waveguide sensor for SO₂ and H₂S detection in the parts-per-trillion regime using tetraaminophenyl porphyrin," *Journal of Modern Optics*, 2020, 67(6): 1–8.

[10] G. Tuerdi, N. Kari, Y. Yan, P. Nizamidin, and A. Yimit, "A functionalized tetrakis(4-Nitrophenyl)porphyrin film optical waveguide sensor for detection of H₂S and ethanediamine gases," *Sensors*, 2017, 17(12): 2717.

[11] Y. W. Huang, S. K. Kalyoncu, Q. Zhao, R. Torun, and O. Boyraz, "Silicon-on-sapphire waveguides design for mid-IR evanescent field absorption gas sensors," *Optics Communications*, 2014, 313: 186–194.

[12] N. L. Kazanskiy, S. N. Khonina, and A. Butt, "Polarization-insensitive hybrid plasmonic waveguide design for evanescent field absorption gas sensor," *Photonic Sensors*, 2020, DOI: 10.1007/s13320-020-0601-6.

[13] S. N. Khonina, N. L. Kazanskiy, and A. Butt, "Evanescent field ratio enhancement of a modified ridge waveguide structure for methane gas sensing application," *IEEE Sensors Journal*, 2020, 20(15): 8469–8476.

[14] C. Ranacher, C. Consan, N. Vollert, A. Tortschanoff, M. Bergmeister, T. Grille, *et al.*, "Characterization of evanescent field gas sensor structures based on silicon photonics," *IEEE Photonics Journal*, 2018, 10(5): 1–14.

[15] A. Y. Mironenko, A. A. Sergeev, A. E. Nazirov, E. B. Modin, S. S. Voznesenskiy, and S. Y. Bratskaya, "H₂S optical waveguide gas sensors based on chitosan/Au and chitosan/Ag nanocomposites," *Sensors and Actuators B: Chemical*, 2016, 225: 348–353.

[16] Y. Yan, P. Nizamidin, G. Turdi, N. Kari, and A. Yimit, "Room-temperature H₂S gas sensor based on au-doped ZnFe₂O₄ yolk-shell microspheres," *Analytical Sciences the International Journal of the Japan Society for Analytical Chemistry*, 2017, 33(8): 945–951.

[17] A. Abdukayum, A. Yimit, M. Mahmut, and K. Itoh, "A planar optical waveguide sensor for hydrogen sulfide detection," *Sensor Letters*, 2007, 5(2): 395–397.

[18] Q. R. Ma, B. Kutluk, N. Kari, S. Abliz, and A. Yimit,

"Study on surface sensitization of g-C₃N₄ by functioned different aggregation behavior porphyrin and its optical properties," *Materials Science in Semiconductor Processing*, 2021, 121: 105316.

[19] R. Olgac, T. Soganci, Y. Baygu, Y. A. Gok, and M. Ak, "Zinc(II) phthalocyanine fused in peripheral positions octa-substituted with alkyl linked carbazole: Synthesis, electropolymerization and its electro-optic and biosensor applications," *Biosensors and Bioelectronics*, 2017, 98: 202–209.

[20] P. Khoza, I. Ndhundhuma, A. Karsten, and T. Nyokong, "Photodynamic therapy activity of phthalocyanine-silver nanoparticles on melanoma cancer cell," *Journal of Nanoscience and Nanotechnology*, 2020, 20(5): 3097–3104.

[21] P. Sen, M. Managa, and T. Nyokong, "New type of metal-free and Zinc(II), In(III), Ga(III) phthalocyanines carrying biologically active substituents: synthesis and photophysicochemical properties and photodynamic therapy activity," *Inorganica Chimica Acta*, 2019, 491: 1–8.

[22] F. Chen, K. Li, and G. Hu, "Catalytic oxygen reduction property of carbon nanotubes supported tetra-nitro-metal phthalocyanines-MnO₂ dual catalysts," *Chinese Journal of Applied Chemistry*, 2019, 36(1): 97–106.

[23] Z. O. Makinda, M. S. Louzada, J. Britton, T. Nyokong, and S. Khene, "Spectroscopic and nonlinear optical properties of alkyl thio substituted binuclear phthalocyanines," *Dyes and Pigments*, 2019, 162: 249–256.

[24] J. W. Shi, L. Q. Luan, W. J. Fang, T. Y. Zhao, W. Liu, and D. L. Cui, "High-sensitive low-temperature NO₂ sensor based on Zn (II) phthalocyanine with liquid crystalline properties," *Sensors and Actuators B: Chemical*, 2014, 204: 218–223.

[25] X. H. Liang, Z. M. Chen, H. Wu, L. X. Guo, C. Y. He, B. Wang, *et al.*, "Enhanced NH₃-sensing behavior of 2,9,16,23-tetrakis (2,2,3,3-tetrafluoropropoxy) metal(II) phthalocyanine/multi-walled carbon nanotube hybrids: An investigation of the effects of central metals," *Carbon*, 2014, 80: 268–278.

[26] T. Miyata, S. Kawaguchi, M. Ishii, and T. Minami, "High sensitivity chlorine gas sensors using Cu-phthalocyanine thin films," *Thin Solid Films*, 2003, 425(1–2): 255–259.

[27] S. Senthilarasu, S. Velumani, R. Sathyamoothr, A. Subbarayan, J. A. Ascencio, G. Ganizal, *et al.*, "Characterization of zinc phthalocyanine (ZnPc) for photovoltaic applications," *Applied Physics A*, 2003, 77(3–4): 383–389.

[28] T. P. Mthethwa, S. Tuncel, M. Durmus, and T. Nyokong, "Photophysical and photochemical properties of a novel thiol terminated low symmetry zinc phthalocyanine complex and its gold nanoparticles conjugate," *Dalton Transactions*, 2013,

42(14): 4922–4930.

[29] Z. Q. Song, Q. X. Tang, Y. H. Ton, and Y. C. Liu, "High-response identifiable gas sensor based on a gas-dielectric ZnPc nanobelt FET," *IEEE Electron Device Letters*, 2017, 38(11): 1586–1589.

[30] T. P. Lei, Y. B. Shi, W. L. Lu, L. Yang, T. Wei, P. L. Yuan, *et al.*, "Chlorine gas sensors using hybrid organic semiconductors of PANI/ZnPcCl$_{16}$," *Journal of Semiconductors*, 2010, 31(8): 084010.

[31] P. Nizamidin, A. Yimit, I. Nurulla, and K. Itoh, "Optical waveguide BTX gas sensor based on yttrium-doped lithium iron phosphate thin film," *International Scholarly Research Notices*, 2014, 2012(12): 1–6.

[32] A. Ogunsipe and T. Nyokong, "Effects of substituents and solvents on the photochemical properties of zinc phthalocyanine complexes and their protonated derivatives," *Journal of Molecular Structure*, 2004, 689(1–2): 89–97.

[33] B. Ghanbari, L. Shahhoseini, N. Mahlooji, P. Gholamnezhad, and R. Z. Taheri, "Through-space electronic communication of zinc phthalocyanine with substituted [60]fullerene bearing O$_2$Nxaza-crown macrocyclic ligands," *Spectrochimica Acta Part A: Molecular and Biomolecular Spectroscopy*, 2017, 171: 330–339.

[34] X. J. Liu, C. Qi, T. Bing, X. H. Cheng, and D. H. Shangguan, "Highly selective phthalocyanine-thymine conjugate sensor for Hg^{2+} based on target induced aggregation," *Analytical Chemistry*, 2009, 81(9): 3699–3704.

[35] J. X. Yi, Z. H. Chen, J. H. Xiang, and F. S. Zhang, "Photocontrollable J-aggregation of a diarylethene-phthalocyanine hybrid and its aggregation- stabilized photochromic behavior," *Langmuir*, 2011, 27(13): 8061–8066.

[36] J. M. Wang, P. Nizamidin, Y. Zhang, N. Kari, and A. Yimit, "Detection of trimethylamine based on a manganese tetraphenylporphyrin optical waveguide sensing element," *Analytical Sciences*, 2018, 34(5): 559–565.

[37] A. Ogunsipe and T. Nyokong, "Effects of substituents and solvents on the photochemical properties of zinc phthalocyanine complexes and their protonated derivatives," *Journal of Molecular Structure*, 2004, 689(1–2): 89–97.